type of infantile-onset ascending spastic paralysis with bulbar involvement in two siblings. Clin Genet 2003；64：210—215

8) Otomo A, Hadano S, Okada T, et al：ALS2, a novel guanine nucleotide exchange factor for the small GTPase Rab5, is implicated in endosomal dynamics. Hum Mol Genet 2003；12：1671—1687

Abstract

Recessive motor neuron diseases：Mutations in the ALS2 gene and molecular pathogenesis for the upper motor neurodegeneration

Joh-E Ikeda, Ph.D.
Tokai University, Graduate School of Medicine, Neurodegenerative Diseases Research Centre

We have initially identified a mutation in ALS2 as a causative for a juvenile autosomal recessive form of amyotrophic lateral sclerosis（ALS）, termed ALS2（OMIM 205100）. ALS2 mutations also are causative for an autosomal recessive juvenile primary lateral sclerosis, and infantaile-ascending hereditary spastic paralysis. To date, nine homozygous ALS2 mutaions from nine independent families have been identified. All of these mutations result in predicted premature translation termination caused by the recessive frameshift or nonsense mutation. ALS2 is a 184-kD protein comprising several putative guanine nucleotide exchange factor（GEF）domains [RLD；RCC1 like domain, DH, PH domain, VPS9；Vacuolar protein sorting 9 domain]. In vitro, ALS2 specifically binds to the small GTPase Rab5 and functions as a GEF for Rab5. Ectopic expression of full-length ALS2 has further implied an association with endosomal membranes mediated by the VPS9 domain, consistent with ALS2 involvement in endosomal trafficking and fusion in conjunction with the activation of Rab5. These results combined with our findings suggest that an obstruction of endosomal dynamics might underlie neuronal dysfunction and degeneration in ALS2, PLSJ, and HSP, as well as in a number of other motor neuron diseases.

(Clin Neurol, 44：792—794, 2004)

Key words：familial amyotrophic lateral sclerosis；FALS, ALS2 gene, guanine nucleotide exchange factor；GEF, endosomal dynamics

Journal of Cerebral Blood Flow & Metabolism (2005), 1–13

www.jcbfm.com

A dopamine D4 receptor antagonist attenuates ischemia-induced neuronal cell damage via upregulation of neuronal apoptosis inhibitory protein

Yoshinori Okada[1,2], Harumi Sakai[1], Eri Kohiki[3], Etsuko Suga[3], Yoshiko Yanagisawa[3], Kazunori Tanaka[1], Shinji Hadano[1,3], Hitoshi Osuga[1,3] and Joh-E Ikeda[1,3,4]

[1]*Department of Molecular Neuroscience, The Institute of Medical Sciences, Tokai University, Isehara, Kanagawa, Japan;* [2]*Laboratory for Structure and Function Research, Tokai University School of Medicine, Isehara, Kanagawa, Japan;* [3]*Solution Oriented Research for Science and Technology (SORST), Japan Science and Technology Agency (JST), Tokai University School of Medicine, Isehara, Kanagawa, Japan;* [4]*Department of Paediatrics, University of Ottawa, Ottawa, Ontario, Canada*

Neuronal apoptosis inhibitory protein (NAIP/BIRC1), the inhibitor of apoptosis protein (IAP) family member, suppresses neuronal cell death induced by a variety of insults, including cell death from ischemia and stroke. The goal of the present study was to develop an efficient method for identification of compounds with the ability to upregulate endogenous NAIP and to determine the effects on these compounds on the cellular response to ischemia. A novel NAIP-enzyme-linked immunosorbent assay (ELISA)-based *In vitro* drug-screening system is established. Use of this system identified an antagonist of dopamine D4 receptor, termed L-745,870, with a potent NAIP upregulatory effect. L-745,870-mediated NAIP upregulation in neuronal and nonneuronal cultured cells resulted in decreased vulnerability to oxidative stress-induced apoptosis. Reducing NAIP expression via RNA interference techniques resulted in prevention of L-745,870-mediated protection from oxidative stress. Further, systemic administration of L-745,870 attenuated ischemia-induced damage of the hippocampal CA1 neurons and upregulated NAIP expression in the rescued hippocampal CA1 neurons in a gerbil model. These data suggest that the NAIP upregulating compound, L-745,870, has therapeutic potential in acute ischemic disorders and that our NAIP-ELISA-based drug screening may facilitate the discovery of novel neuroprotective compounds.
Journal of Cerebral Blood Flow & Metabolism advance online publication, 23 February 2005; doi:10.1038/sj.jcbfm.9600078

Keywords: antiapoptosis; dopamine receptor antagonist; IAP; ischemia; NAIP; oxidative stress

Introduction

Several studies have demonstrated that the mechanisms of ischemia-induced neuronal cell death fall on the continuum between necrosis and apoptosis (Raghupathi *et al*, 2000; Graham and Chen, 2001). While relatively more interest has been focused on prevention of cell necrosis after ischemic insults, apoptosis, with its ordered series of events, including caspase activation (Graham and Chen, 2001) and/or the perturbation of calcium homeostasis (Love, 1999), may represent a more suitable target for modulation for the goal of preventing cell death. This may be particularly true for neuronal damage after cerebral ischemia (Nitatori *et al*, 1995).

Recent studies have demonstrated that various antiapoptotic proteins, including Bcl-2, neuronal apoptosis inhibitory protein (NAIP, also called baculoviral IAP repeat-containing 1 (BIRC1)), and X-linked inhibitor of apoptosis (XIAP), are upregulated in neurons after ischemia (Graham and Chen, 2001; Krajewski *et al*, 1995; Xu *et al*, 1997, 1999). Among these antiapoptotic proteins, NAIP, the founding member of the inhibitor of apoptosis protein (IAP) family, was identified in the course

Correspondence: Dr J-E Ikeda, Department of Molecular Neuroscience, The Institute of Medical Sciences, Tokai University, Isehara, Kanagawa 259-1193, Japan.
E-mail: jei@m.med.u-tokai.ac.jp
This work was funded by the Japan Science and Technology Agency (JST). A part of the work was supported by a Grant-in-Aid for Scientific Research on Priority(C)-Advanced Brain Science Project from the Ministry of Education, Culture, Sports, Science, and Technology of Japan.
Received 4 August 2004; revised 15 November 2004; accepted 6 December 2004

of the positional cloning of the gene responsible for spinal muscular atrophy (SMA) (Roy *et al*, 1995). In actuality, the primary genetic defect in SMA results from mutations in an adjacent gene, survival motor neurons (SMN). However, patients with the most severe form of SMA have large deletions that encompass both the *SMN* and *NAIP* genes. These data suggest that NAIP may also play a role in neuronal viability (Gavrilov *et al*, 1998; Hsieh-Li *et al*, 2000; Monani *et al*, 2000).

Indeed, overexpression of NAIP by adenovirus-mediated gene transfer reduces ischemic cell damage in the rat hippocampus (Xu *et al*, 1997). Further, ectopic NAIP expression rescues motor neurons after peripheral nerve axotomy (Perrelet *et al*, 2000) and preserves nigrostriatal dopaminergic function in the intrastriatal 6-hydroxydopamine (6-OHDA) rat model of Parkinson's disease (Crocker *et al*, 2001). Moreover, NAIP promotes motor neuron survival through the intracellular signaling of glial cell-derived neurotrophic factor (GDNF) (Perrelet *et al*, 2002). Finally, unlike other IAP proteins and Bcl-2 family proteins, NAIP exerts a unique antiapoptotic activity against oxidative stresses. These findings suggest that NAIP plays an important role in the protection of the neuronal cells from apoptotic insults, and that upregulation of endogenous NAIP may represent a therapeutic approach for prevention of oxidative stress-induced neuronal cell damage.

Therefore, the goal of the present study was to develop an efficient method for identification of compounds with the ability to upregulate endogenous NAIP and to determine the effects of these compounds on the cellular response to ischemia.

Materials and methods

Chemicals

A total of 953 compounds, including 3-[(4-[4-chlorophenyl]piperazine-1-yl)methyl]-[1H]-pyrrolo[2,3-*b*] pyridine-trihydrochloride (L-745,870) listed in 'Neurochemicals, Signal Transduction Agents, Pharmacological Probes and Biochemicals compounds; Tocris Cookson Ltd', was purchased from Tocris Cookson Ltd (Bristol, UK) and subjected to drug-screening experiments. Drug concentrations were tested in a range from 1 to 100 μmol/L. All other cytotoxins including menadione, H_2O_2, α-naphthoquinone, 2,3-dimethoxy-1,4-naphthoquinone (DMNQ), actinomycin D, staurosporine, *cis*-platinum, okadaic acid, oligomycin, and etoposide were purchased from Sigma-Aldrich (St Louis, MO, USA).

Antibodies

Two independent anti-human NAIP antibodies, IB9 and ME1, were generated. IB9, a mouse monoclonal antibody, was raised using an epitope of the human NAIP C-terminal peptide (amino acids 841 to 1052), and a polyclonal antibody, ME1 (1:3,000 dilution), was obtained by immunizing rabbits with recombinant NAIP peptide (amino acids 256 to 587). ME1 recognizes the BIR3 region of NAIP and crossreacts with the mouse and gerbil NAIP proteins (data not shown). Other antibodies used in this study included rabbit polyclonal anti-XIAP antibody (#AF822; 1:1,000; R&D Systems, Minneapolis, MN, USA), rabbit polyclonal anti-cIAP-1 antibody (#AF818; 1:1,000; R&D Systems), rabbit polyclonal anti-cIAP-2 antibody (#AF817; 1:1,000; R&D Systems), rabbit polyclonal anti-Survivin antibody (#NB500-201; 1:1,000; Novus Biologicals, Littleton, CO, USA), rabbit polyclonal anti-Bcl-2 antibody (#SC-783; 1:1,000; Santa Cruz Biotechnology, CA, USA), rabbit polyclonal anti-Bcl-xL antibody (#SC-634; 1:1,000; Santa Cruz Biotechnology), and mouse monoclonal anti-β-tubulin antibody (#SC-5274; 1:50,000; Santa Cruz Biotechnology).

Cell Lines and Culture Conditions

The human monocyte-derived cell line, THP-1, was cultured in RPMI-1640 (Invitrogen, Carlsbad, CA, USA), while HeLa and SH-SY5Y neuroblastoma cells were cultured in Dulbecco's modified Eagle's medium (DMEM) (Invitrogen). All culture media contained penicillin (50 IU/mL) and streptomycin (50 μg/mL) and were supplemented with 10% fetal calf serum. SH-SY5Y cells, which were seeded with a density of 4×10^5 cells/well in six-well plates, were differentiated by treatment with all-*trans*-retinoic acid (Tocris Cookson) at a concentration of 10 μmol/L.

NAIP-ELISA and Screening of NAIP Upregulating Compounds

NAIP-neuronal apoptosis inhibitory protein-enzyme-linked immunosorbent assay (ELISA)-based screening with THP-1 cells was conducted to identify compounds that induced endogenous NAIP expression. THP-1 cells were cultured in 24-well plates at a density of 2×10^5 cells/well for 24 h, followed by incubation in the presence of tested compounds for either 24 or 72 h. Cells were then lysed with NP40 buffer (50 mmol/L Tris-HCl, pH 7.5, 150 mmol/L NaCl, 1% NP40, and protein inhibitor cocktail (Complete; Roche Diagnostics, Indianapolis, IN, USA)). Aliquots of extracts were subjected to the NAIP-ELISA assay, with 1B9 as primary antibody conjugated to the ELISA plate and with ME1 as secondary antibody for quantification of NAIP immunoreactivity. Assays were conducted according to standard ELISA procedure (Crowther, 1995).

Western Blot Analysis

The extracts from cultured cells were electrophoretically separated on 5% to 20% SDS-polyacrylamide gels and transferred onto polyvinylidene difluoride (PVDF) membranes (Bio-Rad Laboratories, Hercules, CA, USA). Membranes were then incubated with the indicated primary antibodies in TBST buffer (50 mmol/L Tris-HCl; pH 7.4, 150 mmol/L NaCl, 0.1% (w/v) Tween-20) for 2 h, after

incubation with the peroxidase-linked secondary anti-rabbit IgG (#NA934; Amersham Pharmacia Biotech, Uppsala, Sweden) or anti-mouse IgG (#NA931; Amersham Pharmacia Biotech) antibody for 1 h. Signals were detected using ECL Plus (Amersham Pharmacia Biotech).

Cell Viability Assay

Approximately 1×10^5 cells, which were either pretreated with 10 μmol/L of L-745,870 for 24 h or left untreated, were plated on a 96-well plate and incubated for 5 h at 37°C. The appropriate amounts of the cytotoxins, including free radical generating compounds (DMNQ: 120 μmol/L, menadione: 20 to 80 μmol/L, α-naphthoquinone: 60 μmol/L and H_2O_2: 30 μmol/L), kinase inhibitor (staurosporine: 1 nmol/L), ATPase inhibitor (oligomycin: 100 μmol/L), DNA-damaging reagent (*cis*-platinum: 100 μmol/L), phosphatase inhibitor (okadaic acid: 100 nmol/L), and topoisomerase II inhibitors (actinomycin D: 1 μmol /L and etoposide: 100 μmol/L), were added, and the preparation was allowed to incubate for another 1 to 10 h. The medium was then replaced with fresh medium containing 10% (v/v) alamarBlue (AccuMed International, Westlake, OH, USA), followed by incubation for an additional 4 h at 37°C. Cell numbers were counted fluorometrically as per the alamarBlue Assay instructions.

Flow-Cytometric Analysis of Apoptotic/Necrotic Cell Death

Quantification of the apoptotic/necrotic cell death was performed by flow cytometry in conjunction with the MEBCYTO Apoptosis Kit (MBL, Nagoya, Japan). In brief, HeLa cells that were pretreated with or without L-745,870 were plated on a six-well plate (3×10^5 cells/well). After 4 h of incubation, menadione (or H_2O_2) was added to the cells, followed by incubation for an additional 4 h (or 40 mins for H_2O_2). The cells were washed once with phosphate-buffered saline (PBS) and suspended in fresh medium for Annexin V-FITC and propidium iodide (PI) labeling, which was performed according to the manufacturer's instructions (MBL). The cells were sorted and analyzed by FACScan (Beckton Dickinson, San Jose, CA, USA). Cell damage was classified according to the extent of staining of AnnexinV-FITC and PI (Quadrant analysis). Quadrants were comprised of the upper left (UL; AnnexinV−/PI+), upper right (UR; AnnexinV+/PI+), low left (LL; AnnexinV−/PI−), and low right (LR; AnnexinV+/PI−). LL, LR, and UR represent the cells in normal state, early stage of apoptosis, and late stage of apoptosis/necrosis, respectively.

RNA Interference

Neuronal apoptosis inhibitory protein RNA interference (RNAi) was achieved by expressing the hairpin-forming short RNA molecules generated from a portion of the 3′UTR of the human *NAIP/BIRC1* gene. Briefly, 19-nucleotide-long inverted repeats, 5′-GTCAACTCCCCT-CCCCTTG-3′ (sense) and 5′-CAAGGGGAGGGGAGTT-GAC-3′ (antisense), which were intervened with the 9-nucleotide spacer (TTCAAGAGA), were inserted downstream of the U6 promoter of pSilencer 1.0-U6 vector (Ambion, Austin, TX, USA), generating pSilencer 1.0-U6-NAIP. HeLa cells, which were either pretreated with L-745,870 for 24 h or left untreated, were cotransfected with 10 μg of pSilencer 1.0-U6-NAIP and 1 μg of pMACS K^k.II (Miltenyi Biotec, Bergisch Gladbach, Germany) using FuGENE6 (Roche Diagnostics). After 48 h, the transfected cells were magnetically enriched and cultured for 24 h. NAIP expression and cell viability were analyzed by Western blotting and by the alamarBlue Assay, respectively.

Generation of Forebrain Ischemic Model in Gerbils

All animal experimental procedures were performed in accordance with the guidelines of the Tokai University School of Medicine Committee on Animal Care and Use. Twelve-week-old Male Mongolian gerbils (Clea Japan Inc., Tokyo, Japan), weighing 70 to 80 g, were used. Animals were anesthetized with halothane (4%) in a mixture of N_2O/O_2 (70:30) initially, and halothane was gradually decreased to 2% for maintenance of anesthesia during surgery. Under anesthesia, a femoral artery catheter was placed to monitor mean arterial blood pressure, and rectal and temporal muscle temperatures were monitored and maintained at 37°C±0.5°C via a heating pad and radiant heat during and after surgery. Forebrain ischemia was induced by bilateral common carotid artery occlusion (BCCAO) using 3-mm sugita-aneurysm clips (Kirino and Sano, 1984). After 10 mins of occlusion, the aneurysmal clips were removed to allow reperfusion, and complete reperfusion of the arteries was verified by direct visual observation. Sham-operated gerbils underwent identical surgery with the exception of the BCCAO procedure. Under these experimental conditions, in which a relatively severe ischemic condition was used, all animals survived until fixation.

To investigate the *in vivo* effect of L-745,870 (Tocris Cookson Ltd) on ischemia-induced cell death, the compound was dissolved in physiologic saline and was administered to gerbils at a dose of 7 mg/kg ($n=6$), 70 mg/kg ($n=7$), 140 mg/kg ($n=7$), or 210 mg/kg ($n=6$). We have administered the compound to the animals 1 h before ischemic surgery to ensure the protection of neurons from the oxidative stress-induced cell death. This experimental protocol was designed based on the *in vitro* experimental data in which the pretreatment with the compound effectively protects cultured cells from the menadione-induced insults (refer to Figures 1 to 4). Administration of the compound was performed intragastrically via oral cannula under anesthesia. Vehicle-treated animals ($n=7$) received physiologic saline alone. Sham-operated animals ($n=3$) were administered with a compound dose of 210 mg/kg.

Measurement of Regional Cerebral Blood Flow

To analyze the effect of the compound on regional cerebral blood flow (CBF), a subset of animals underwent measure-

ment of CBF at 2 and 24 h after administration of L-745,870 (210 mg/kg) or vehicle. Cerebral blood flow was measured by the hydrogen clearance method via a platinum wire electrode stereotaxically inserted into the right hippocampus using coordinates of 2 mm posterior and 2 mm lateral to the bregma, and 2.5 mm below the brain surface in a flat cranial presentation, as previously reported (Osuga *et al*, 2000).

Histopathology

After 3 days of reperfusion, animals were anesthetized with 4% halothane and perfused with 60 mL of 4% paraformaldehyde in phosphate buffer (pH 7.4) via a catheter placed in the heart. The brains were removed, fixed in 10% formalin for 10 days, and embedded in paraffin. Paraffin sections were sliced at a thickness of 7 μm for histopathologic and immunohistochemical evaluation. Neuronal cell density of the CA1 subfield of the hippocampus, that is, the number of intact CA1 pyramidal neurons per 1 mm linear length of pyramidal cell layer, was measured by counting 7 μm sections stained with hematoxylin and eosin from 3 to 7 independent animals in a double-masked manner.

Immunohistochemistry

Brain sections were subjected to NAIP and XIAP immunohistochemistry with polyclonal anti-human NAIP (ME1) and XIAP antibodies (R&D Systems Inc.), respectively, and stained using the Vectastain elite ABC kit (Vector Laboratories Inc., Burlingame, CA, USA) according to the manufacturer's instructions. In brief, after deparaffinization, the sections were washed with 0.01 mol/L PBS (pH 7.2) for 5 mins and were incubated with anti-NAIP (5 μg/mL) or anti-XIAP (5 μg/mL) antibody overnight at 4°C. The sections were rinsed three times with PBS containing 0.05% Triton X-100 for 10 mins, incubated with biotinylated secondary antibody for 3 h, and then incubated with avidin–biotin–peroxidase complex for 1 h at room temperature. Finally, the sections were treated with 0.5% 3,3′-diaminogenzidine (DAB) and 0.01% H_2O_2 in Tris-HCl buffer (pH 7.5), and the DAB reaction products were observed under a microscope.

Statistical Analysis

All data in this study are presented as mean ± s.e. Data were analyzed for significance using Student's *t*-test for pair-wised comparisons or ANOVA followed by Scheffe's test for multiple comparisons between groups (Statview 5.0 software; SAS, Cary, NC, USA). A *P*-value <0.05 was considered as reaching statistical significance.

Results

Identification of NAIP Upregulating Compounds

To identify compounds with the ability to induce NAIP expression, 953 compounds (Tocris) were screened using NAIP-ELISA. Compounds were arbitrarily categorized as 'downregulator' ($n=16$) if the resulting NAIP level was less than 70% of the normal endogenous level (i.e., ~12 ng/mL), or 'upregulator' ($n=30$) if the resulting NAIP level was more than 200% of the normal endogenous NAIP level (Table 1).

To examine whether the 30 identified NAIP upregulators suppressed menadione-induced cell death, THP-1 cell viability assays were performed in cells pretreated with menadione followed by the addition of each NAIP upregulator. All 30 compounds exerted a protective effect against menadione-induced cell death with variable degrees (Table 1). The compound that exerted the most potent protective effect was L-745,870, a dopamine D4 receptor antagonist (Figure 1A). This compound was used for subsequent experiments.

L-745,870 Protects a Variety of Cultured-Cells Against Menadione-Induced Cell Death

To determine whether the protective effect of L-745,870 on THP-1 cells was specific to cell type, cell viability studies were also conducted in HeLa and SH-SY5Y (differentiated neuroblastoma by all-*trans*-retinoic acid treatment) cells after exposure to the compound. L-745,870 protected both cell lines from menadione-induced cell death (Figures 1A, THP-1; B, HeLa; and C, SH-SY5Y). Further, the dose-

Table 1 Screening of 953 Tocris compounds by NAIP-ELISA, and viability assays after challenging with menadione-induced oxidative stress in THP-1 cells

NAIP level	*NAIP concentration*			*Cell viability (%)*
	Mean ± s.e. (ng/mL)	*Minimum (ng/mL)*	*Maximum (ng/mL)*	*(n) (menadione; 40 μmol/L)*
Untreated (control)	12.4 ± 0.3 (240)	11.8	12.7	31–37% (30)
Compound treated				
Unchanged	12.9 ± 0.4 (907)	10.1	21.3	ND*
Upregulator	54.8 ± 12.1 (30)	31.8	78.8	45–93% (30)
Downregulator	8.6 ± 0.8 (16)	7.1	9.1	ND*

NAIP, neuronal apoptosis inhibitory protein; ELISA, enzyme-linked immunosorbent assay; *ND, not determined. Number in each parenthesis indicates the number of tested compounds.

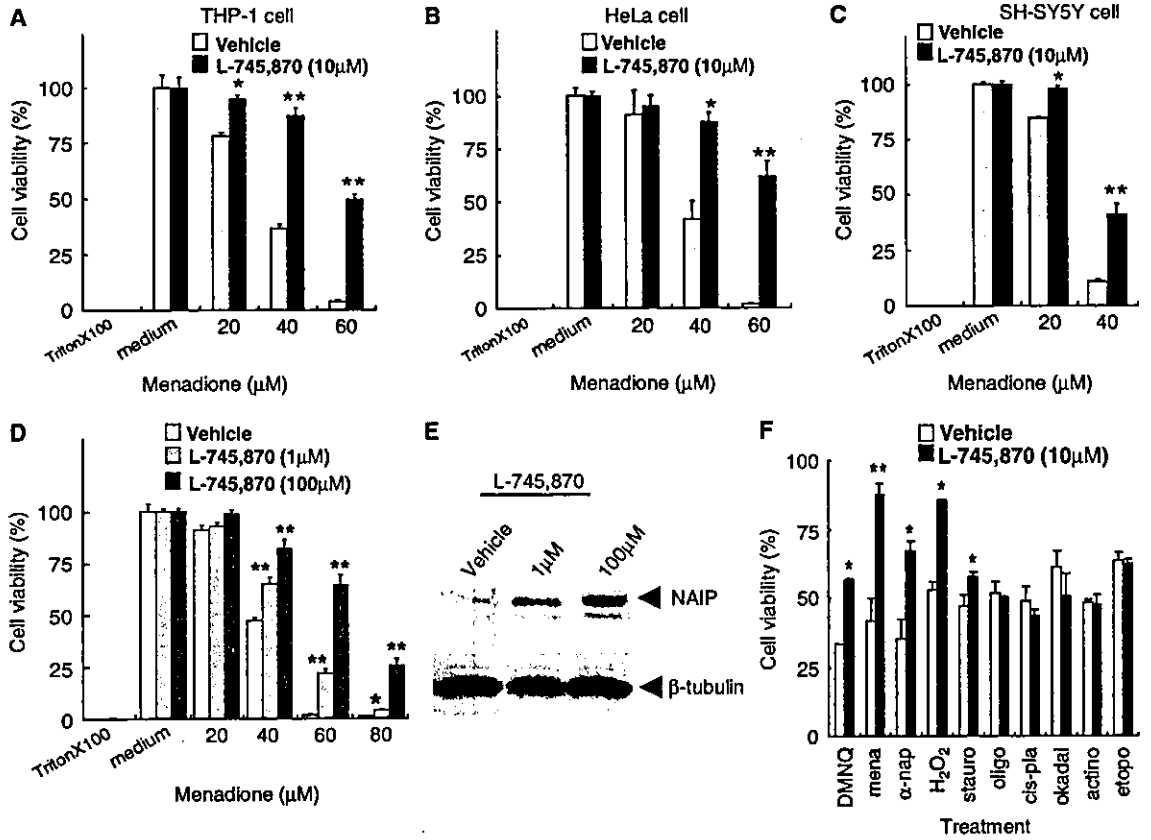

Figure 1 The effect of L-745,870 on oxidative stress-induced cell death. Cell viability after menadione treatment in **(A)** THP-1, **(B)** HeLa, and **(C)** differentiated SH-SY5Y cells was assayed. Cells that were pretreated with vehicle or L-745,870 (10 μmol/L) for 24 h were challenged with menadione (0 to 100 μmol/L) for 4 h. Each value represents the percentages of the cell viability relative to those of control (Triton X-100-treated cells) (means ± s.e.; $n = 8$). $^*P < 0.01$; $^{**}P < 0.001$, versus each corresponding vehicle. Statistical analysis was performed using Student's *t*-test. **(D** and **E)** Effect of various concentrations of L-745,870 on neuronal apoptosis inhibitory protein (NAIP) expression and cell viability after menadione treatment in HeLa cells. **(D)** Cells were pretreated with vehicle or L-745,870 (1 and 100 μmol/L) for 24 h and then challenged with menadione (0 to 100 μmol/L) for 4 h. $^*P < 0.01$; $^{**}P < 0.001$, versus each corresponding vehicle. Statistical analysis was performed using ANOVA with Scheffe's *post hoc* test. **(E)** Western blotting analysis of NAIP in HeLa cells treated with L-745,870 (1 and 100 μmol/L) or vehicle for 24 h. The arrowhead indicates the position of NAIP (150 kDa). Expression of β-tubulin was not affected by L-745,870 treatment and shows that equal amount of proteins loaded in each lane of the blot. **(F)** Effects of L-745,870 on cell viability after exposure to cell death-inducing agents in HeLa cells. Cells were pretreated with vehicle or L-745,870 (10 μmol/L) for 24 h and then exposed to various reagents, including DMNQ, menadione (mena), α-naphthoquinone (α-na), H_2O_2, staurosporine (stauro), oligomycin (oligo), *cis*-platinum (*cis*-pla), okadaic acid (okadaic), actinomycin D (actino), and etoposide (etopo). $^*P < 0.01$; $^{**}P < 0.001$, versus each corresponding vehicle. Statistical analysis was performed using Student's *t*-test.

dependent increase in cell viability correlated with a concomitant increase in NAIP level in HeLa cells (Figures 1D and 1E).

L-745,870 Selectively Protects Cells Against Oxidative Stress-Induced Apoptosis

To gain insight into the suppression of the cell death with L-745,870, HeLa cells pretreated with L-745,870 were challenged with various apoptosis-inducing stimuli and chemical cell-stressors. L-745,870 specifically suppressed cell death induced by oxidative stressors, including cell death in response to menadione, hydrogen peroxide (H_2O_2), DMNQ, and α-naphthoquinone, but did not protect against cell death induced by nonoxidative stressors (e.g., staurosporine, oligomycin, *cis*-platinum, okadaic acid, actinomycin D, and etoposide) (Figure 1F).

To confirm the antiapoptotic effect of L-745,870 against oxidative stress-induced cell death, flow cytometric analysis of cell treated with L-745,870 and menadione and double-stained with Annexin V-FITC and PI was performed. Half of the population of the menadione-treated cells that were not

exposed to L-745,870 were distributed in the LR quadrant (early stage of apoptosis) in an early phase of incubation (60 mins) but subsequently shifted to the UR quadrant (apoptosis/necrosis) during the late phase of incubation (4 h) (data not shown). These data suggest that cell death in response to menadione is the result of apoptosis rather than necrosis. L-745,870 treatment reduced the apoptotic cell population in the UR quadrant from 45% to 20% and increased the LL and LR quadrant populations from 32% to 59% and 15% to 19%, respectively (Figure 2A). L-745,870 treatment also reduced the apoptotic cell population in the UR quadrant from 78% to 53% and increased the normal cells in the LL quadrant from 6% to 28% in the cells exposed to H_2O_2 for 40 mins (Figure 2B). These results suggest that L-745,870 specifically protects cells from apoptosis induced by oxidative stress.

L-745,870 Specifically Upregulates NAIP

To examine whether L-745,870 specifically induces NAIP expression level among the antiapoptotic proteins, expression levels of the IAP family (XIAP, cIAP-1, cIAP-2, and survivin) and Bcl-2 family (Bcl-2 and Bcl-XL) proteins were assessed in HeLa and SH-SY5Y cells by Western blotting. L-745,870 specifically elevated the endogenous level of NAIP (Figure 3A) but had no effect on the levels of other antiapoptotic proteins (Figures 3B–3G). This observation was consistent with results obtained by the DNAChip analysis (8,300 genes, including all of the known antiapoptotic proteins with the exception of the *NAIP/BIRC1* gene: the Atlas Plastic Arrays analysis; Beckton Dickinson), in which no upregulation of the antiapoptosis relating genes was observed (data not shown). Slight decreases in the levels of XIAP and cIAP-1 were noted only in differentiated SH-SY5Y cells (Figures 3B and 3C), although the physiologic significance for this small effect may not be significant. These results indicate that L-745,870 selectively enhances endogenous NAIP levels.

L-745,870 Inhibits Oxidative Stress-Induced Apoptosis Via NAIP Upregulation

To investigate whether the elevation of the endogenous NAIP level by L-745,870 is responsible for the protection against oxidative stress-induced apoptosis, *NAIP* gene expression was suppressed using NAIP-RNAi. Transfection of HeLa cells with NAIP-U6 resulted in a marked decrease in endogenous NAIP levels (Figure 4A) and a concomitant increase in susceptibility to menadione (Figure 4B). Further, L-745,870-treated/NAIP-U6 transfected HeLa cells showed higher susceptibility to menadione than cells with NAIP-U6 treatment alone (Figure 4B). These results indicate that the increased

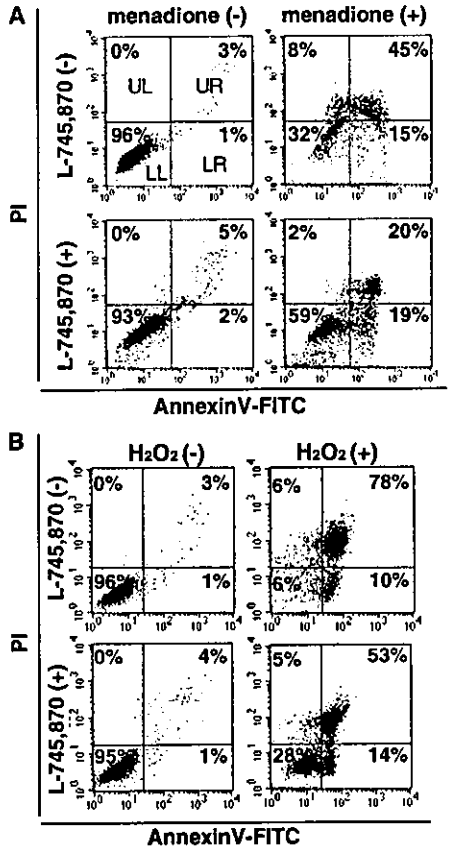

Figure 2 Effect of the neuronal apoptosis inhibitory protein (NAIP) upregulating compound (L-745,870) on the oxidative stress-induced apoptotic cell death, and a flow-cytometric analysis of the apoptotic and/or necrotic cell death in HeLa cells. HeLa cells that were precultured with vehicle or L-745,870 (10 μmol/L) for 24 h were challenged with (A) menadione (+: 50 μmol/L, for 4 h) or (B) H_2O_2 (+: 250 μmol/L, for 40 mins). Cell death was detected by staining with Annexin V-FITC and PI in conjunction with flow cytometry. FACS quadrant analysis allows the classification of the cells into four distinct categories based on the areas in the quadrant: upper left (UL), upper right (UR), low left (LL), and low right (LR). Percentage of the cell numbers in each quadrant is shown on the right.

endogenous NAIP level by L-745,870 likely mediates its ability to protect cells from oxidative stress-induced apoptosis.

Systemic Administration of L-745,870 Results in a Transient Upregulation of NAIP in Gerbil Hippocampal CA1 Neurons

L-745,870 administration had no effect on CBF (control/vehicle; 103.9±13.2 mL/100 g/min, 2 h after administration; 100.3±12.0 mL/100 g/min, and 24 h after administration; 98.9±13.2 mL/100 g/min;

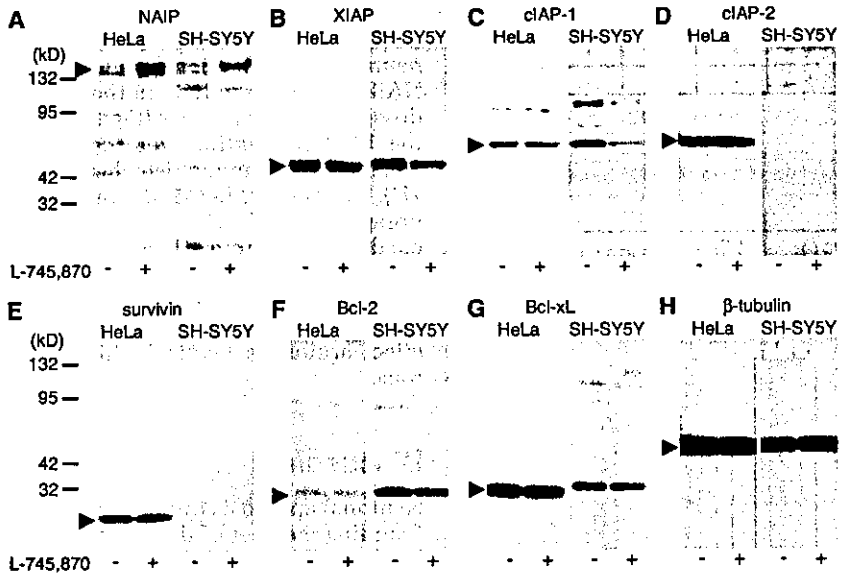

Figure 3 Western blot analysis of antiapoptotic proteins in HeLa and differentiated SH-SY5Y cells after treatment with L-745,870 (+, 10 μmol/L) or vehicle (−) for 24 h. Seven antiapoptotic proteins, including **(A)** neuronal apoptosis inhibitory protein (NAIP), **(B)** X-linked inhibitor of apoptosis (XIAP), **(C)** cIAP-1, **(D)** cIAP-2, **(E)** survivin, **(F)** Bcl-2, and **(G)** Bcl-xL, were analyzed. Each arrowhead indicates the position of each protein (NAIP: 150 kDa, XIAP: 47 kDa, cIAP-1: 65 kDa, cIAP-2: 64 kDa, survivin: 16.5 kDa, Bcl-2: 27 kDa, Bcl-xL: 28 kDa). **(H)** Expression of β-tubulin was not affected by L-745,870 treatment, showing that equal amounts of proteins were loaded in each lane of the blots.

control versus 2 h; $P>0.1$, control versus 24 h; $P>0.1$), blood pressure, and heart rate in gerbils (data not shown), which were consistent with results from a previous study (Patel *et al*, 1999). However, administration of L-745,870 (210 mg/kg) resulted in increased NAIP-immunoreactivity in the hippocampal CA1 neurons at 2 h (Figures 5A and 5B). Further, the increase in NAIP-immunoreactivity peaked at 24 h and then gradually returned to baseline at 72 h after administration (Figures 5A–5D). Results of the Western blotting were consistent with those obtained by the immunohistochemical studies (Figure 5E).

Administration of L-745,870 Attenuates Ischemia-Induced neuronal Cell Death in the Hippocampal CA1 Region

To determine whether administration of L-745,870 exerted neuroprotective against ischemic insults *in vivo*, gerbil forebrain ischemic models were established by transient BCCAO, which induces a selective loss of CA1 pyramidal cells in the hippocampus (Kirino and Sano, 1984). Because the time course of changes in NAIP expression occurred over a 72 h period after administration of L-745,870, the experimental protocol used induction of a relatively severe ischemic condition (10 min BCCAO), followed by the analysis of delayed neuronal loss in the CA1 region over the subsequent 72 h. At 72 h after the ischemic insult, vehicle treated animals showed widespread hippocampal CA1 neuron death with very few surviving neurons present in the pyramidal layer (Figures 6A and 6B). Further, a large number of glial cells were also observed in this area (Figures 6A and 6B). However, these animals showed little or no cell loss in the CA3 region or dentate gyrus (data not shown).

Administration of L-745,870 at 60 mins before the ischemic surgery exerted significant neuroprotective effects against ischemic insults in a concentration-dependent manner. A decreased dosage of L-745,870 (7 mg/kg) showed the most modest protection in the hippocampus CA1 neurons (data not shown), whereas medium to high dosages (70 and 210 mg/kg) exhibited prominent protective effects (Figures 6C–6F). The quantitative scoring of the neuronal cell damage was consistent with these results (Figure 6I). Moreover, the highest dose of L-745,870 (210 mg/kg) was not associated with any CA1 neuron toxicity (Figures 6G and 6H). Further, these protective effects were significant even at 5 days after reperfusion in this experimental condition, despite the fact that progressive cell death in CA1 neurons was observed (data not shown). Together, these results indicate that L-745,870 inhibits progression of the ischemia-induced CA1 neuron death.

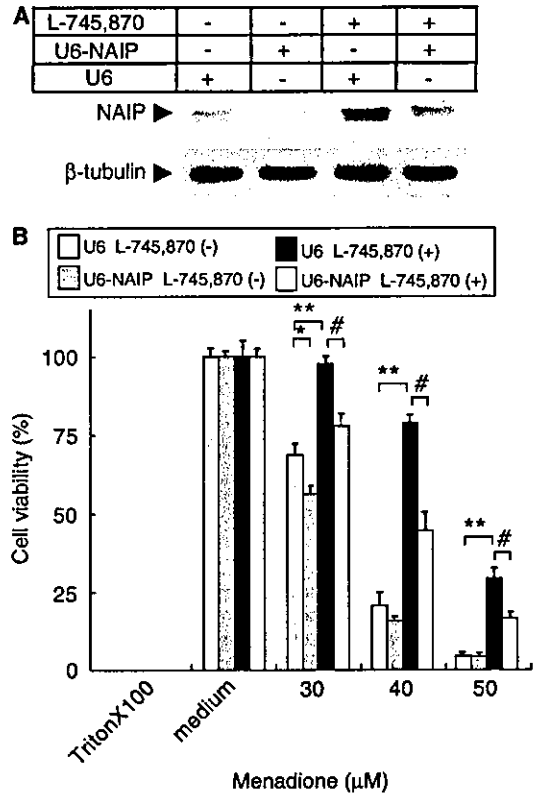

Figure 4 Effect of inhibition of neuronal apoptosis inhibitory protein (NAIP) expression on menadione-induced cell death in HeLa cells. Neuronal apoptosis inhibitory protein RNAi was achieved by ectopically expressing the small interference RNA (siRNA) corresponding to a portion of the 3′-UTR of the *NAIP* gene using the pSilencer 1.0-U6 system. (**A**) Western blot analysis of the NAIP expression in the RNAi treated HeLa cells. The lower panel represents the expression of β-tubulin and showed that equal amounts of protein were loaded in each lane in the blot. (**B**) Effect of the NAIP RNAi on menadione-induced cell death, and on the protection of cell death by L-745,870. Concentration of menadione used in this experiment was between 30 and 50 μmol/L. Cell viability is shown as percentages of the alamarBlue values in U6 or NAIP-U6-transfected cells relative to those of controls (menadione non-treated). Values represent the means ± s.e. of eight independent experiments. $^{*}P<0.01$ and $^{**}P<0.001$ for U6 L-745,870 (−) cells versus NAIP-U6 L-745,870 (+) cells or U6 L-745,870 (+). $^{\#}P<0.001$ for U6 L-745,870 (+) cells versus NAIP-U6 L-745,870 (+) cells. Statistical analysis was performed using Student's *t*-test.

Hippocampal CA1 Neurons Rescued by the Administration of L-745,870 Show Strong NAIP-Immunoreactivity

To investigate whether L-745,870-mediated hippocampal CA1 neuronal protection was associated with elevation of neuronal NAIP levels, immunohistochemical and Western blot analyses of endogenous NAIP were performed in CA1 neurons using an NAIP antibody. After 72 h of reperfusion, the CA1 neurons showed significant enhancement of the NAIP-immunoreactivity in the rescued neurons in a dose-dependent manner (Figures 7A–7F). Results of the Western blotting were consistent with results obtained by immunohistochemical studies (Figure 7H). In contrast, L-745,870 produced no detectable upregulation of XIAP-immunoreactivity in the rescued hippocampus (Figures 7G and 7H). These results show that L-745,870 selectively upregulates NAIP *in vivo*, which represent a potential mechanism by which L-745,870 exerts a neuroprotective effect against ischemia in hippocampal CA1 neurons.

Discussion

Neuronal apoptosis inhibitory protein (BIRC1) is the founding member of the IAP family of proteins, and has been shown to inhibit apoptosis of neurons and other types of the cell *in vitro* and *in vivo*. Increases in NAIP, by either viral-mediated NAIP gene transfer or by enhancement of endogenous levels, results in the attenuation of ischemic neuronal cell death (Xu *et al*, 1997). Further, ectopic NAIP expression enhances rescue of motor neurons from peripheral nerve axotomy (Perrelet *et al*, 2000) and leads to preservation of nigrostriatal dopaminergic neurons in the intrastriatal 6-OHDA rat Parkinson's disease model (Crocker *et al*, 2001). Neuronal apoptosis inhibitory protein also contributes to motor neuron survival through intracellular signaling of GDNF (Perrelet *et al*, 2002). Ischemic neuronal injury is associated with excessive generation of reactive oxygen species (ROS) and oxidative stress in the brain (Chan, 1994; Mattson *et al*, 2001; Friedlander, 2003), and the present study showed that NAIP suppresses neuronal cell death by exerting an antiapoptotic function against oxidative stress.

Most tissues and cells, with the exception of hematopoietic tissues, express NAIP in very low levels (Yamamoto *et al*, 1999). Thus, upregulation of endogenous NAIP in neuronal cells may represent a potent therapeutic strategy for prevention of neurodegeneration. Among the 30 NAIP upregulating compounds identified, two compounds, L-745,870 (dopamine D4 receptor antagonist) and bromocriptine (dopamine D2 receptor agonist; data not shown), exerted particularly prominent protection against neurodegeneration in an ischemia gerbil model. A previous study showed that bromocriptine protected neuronal cells from oxidative stress-induced apoptosis (Schapira, 2002), while another study showed that a number of other dopamine D2 receptor agonists attenuated neuronal cell death under ischemic conditions (Liu *et al*, 1995). L-745,870 was originally identified as a specific antagonist for the dopamine D4 receptor and as a drug candidate for antipsychotic treatment because

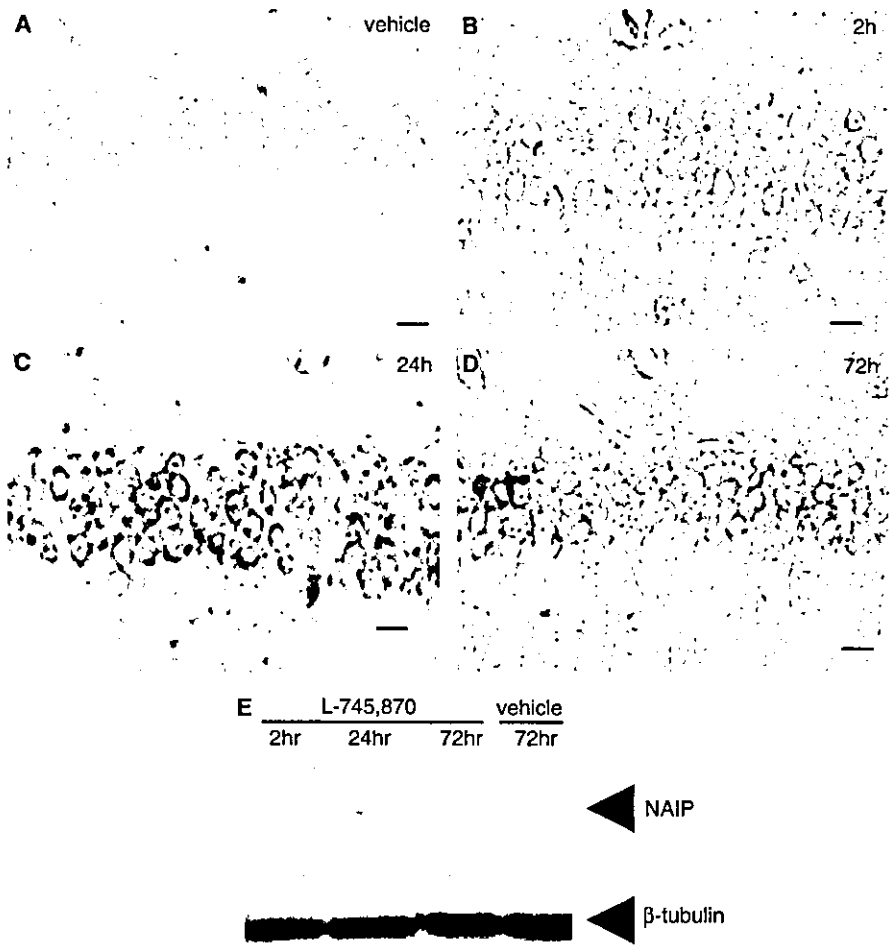

Figure 5 Upregulation of neuronal apoptosis inhibitory protein (NAIP) by L-745,870 in CA1 neurons. Adult gerbils were treated with vehicle (**A**) or L-745,870 (210 mg/kg; **B–D**). Representative coronal brain sections at the level of the dorsal hippocampus at 2, 24, and 72 h after administration of L-745,870 (210 mg/kg) are shown (**B–D**). Tissues were immunostained with the NAIP polyclonal antibody (ME1). Scale bar: 20 μm in higher magnification (× 400; **A–D**). (**E**) Western blot analysis of NAIP in hippocampus at 2, 24, and 72 h (L-745,870; 210 mg/kg) and 72 h (vehicle) after the administration of either L-745,870 or vehicle. Upper and lower panels represent the expression of NAIP and β-tubulin, respectively. Arrows indicate the proteins of interest (NAIP: 150 kDa). Expression of β-tubulin demonstrates equal loading in each lane.

of its excellent oral bioavailability and brain penetration (Patel *et al*, 1997). The present study showed the novel finding that L-745,870 specifically elevated the endogenous NAIP level and enhanced neuronal cell resistance to oxidative stress-induced apoptotic cell death and ischemic neurodegeneration.

The dopamine D4 receptor is a G-protein-coupled receptor that shares sequence homology with the D2 and D3 receptors and is classified as a member of the dopamine D2-like receptors group (Baldessarini, 1997). However, the action of L-745,870 in the present study is likely not mediated via dopaminergic receptors, because the antiapoptotic properties of L-745,870 against oxidative stress-induced cell death were observed in both differentiated dopaminergic SH-SY5Y cells, in which several types of dopamine receptors are expressed (Kamakura *et al*, 1997), and in nonneuronal cells, which do not express these receptors. Indeed, recent reports suggest that the dopamine agonists, bromocriptine and pergolide, act as free radical scavengers (Yoshikawa *et al*, 1994; Sam and Verbeke, 1995; Grünblatt *et al*, 1999) and exert their neuroprotective effects in nonreceptor-mediated fashions (Uberti *et al*, 2002). The present finding that L-745,870

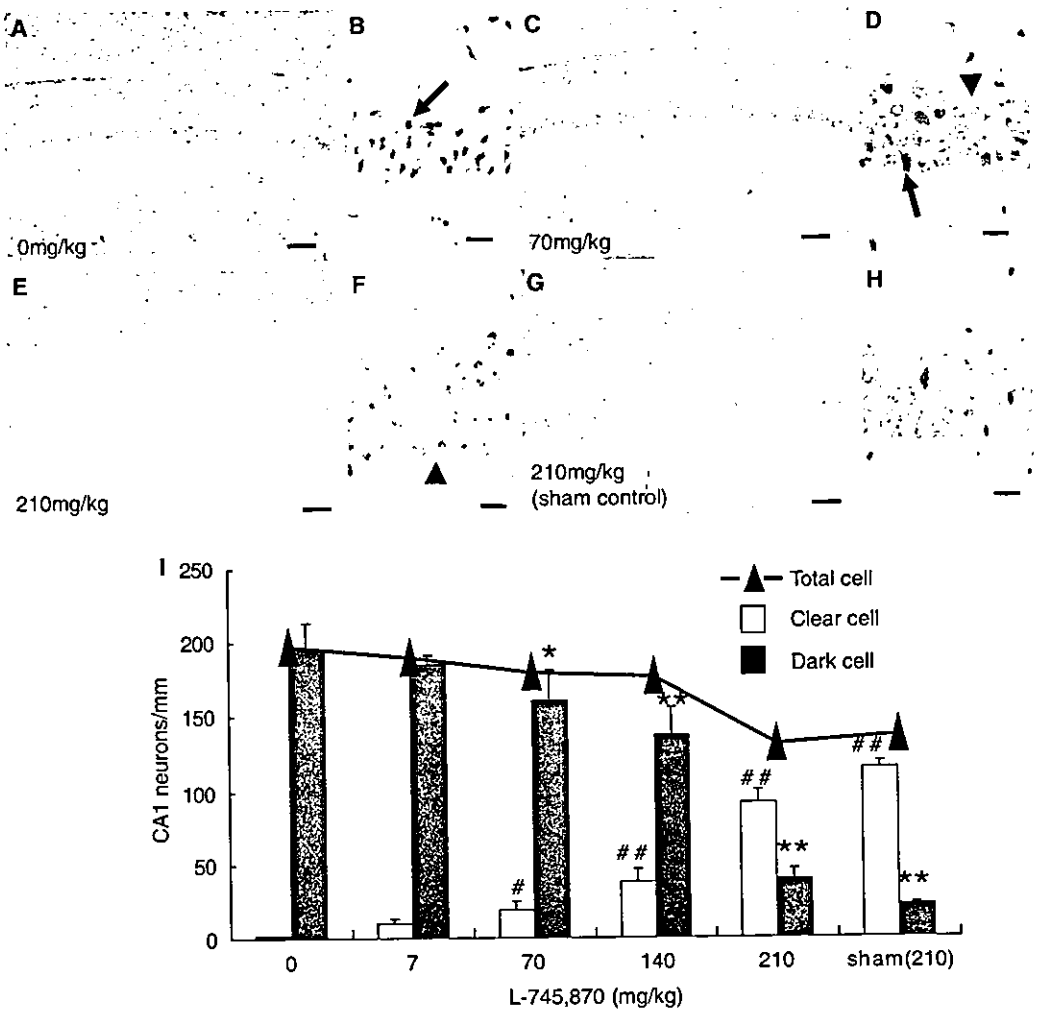

Figure 6 Effects of L-745,870 on ischemia-induced neuronal cell death in gerbils. Adult gerbils were treated with L-745,870 and then subjected to forebrain ischemia (bilateral common carotid artery occlusion (BCCAO) for 10 mins; **A–F**) or sham-operation (**G** and **H**). Representative coronal brain sections at the level of the dorsal hippocampus at 72 h (3 days) after reperfusion are shown. Tissues were stained with hematoxylin–eosin. Dosages of L-745,870 administered were 0 mg/kg (**A** and **B**), 70 mg/kg (**C** and **D**), and 210 mg/kg (**E–H**). Forebrain ischemia resulted in a significant loss of CA1 pyramidal cells. Scale bar: 100 μm in lower magnification (× 100; **A**, **C**, **E**, and **G**); 20 μm in higher magnification (× 400; **B**, **D**, **F**, and **H**). Arrowheads and arrows indicate dark (damaged) and clear (living) cells, respectively. (**I**) Number of pyramidal cells in the CA1 subfield of the hippocampus (cells/mm length of pyramidal cell layer). Both living (clear) and damaged (dark) CA1 neurons were count from six to seven animals in each experiment in a double-masked manner, and the values are represented as means ± s.e. Total numbers of CA1 pyramidal neurons (filled triangles; clear + dark cells) are also shown. $^{*}P<0.01$; $^{**}P<0.001$, compared with dark cells of vehicle-treated control (0 mg/kg). $^{\#}P<0.001$; $^{\#\#}P<0.001$, compared with clear cells of vehicle-treated control (0 mg/kg). Statistical analysis was performed using ANOVA with Scheffe's *post hoc* test.

may exert its neuroprotective via increases in NAIP, either by increasing its expression or stabilization, may provide a mechanism by which all of these effector molecules exert their effects.

The present study showed that L-745,870 upregulated NAIP but not other antiapoptotic proteins. Further, L-745,870 specifically protected both neuronal and nonneuronal cultured cells from apoptosis induced by several oxidative stressors, including DMNQ, menadione, α-naphthoquinone, and H_2O_2. This increase in NAIP likely mediates the protective effect of L-745,870 because reduction of NAIP expression with RNAi inhibited the neuroprotective effect. Recent studies have shown that NAIP suppresses caspase-dependent and -independent apoptosis (Deveraux *et al*, 1997, 1998; Roy *et al*,

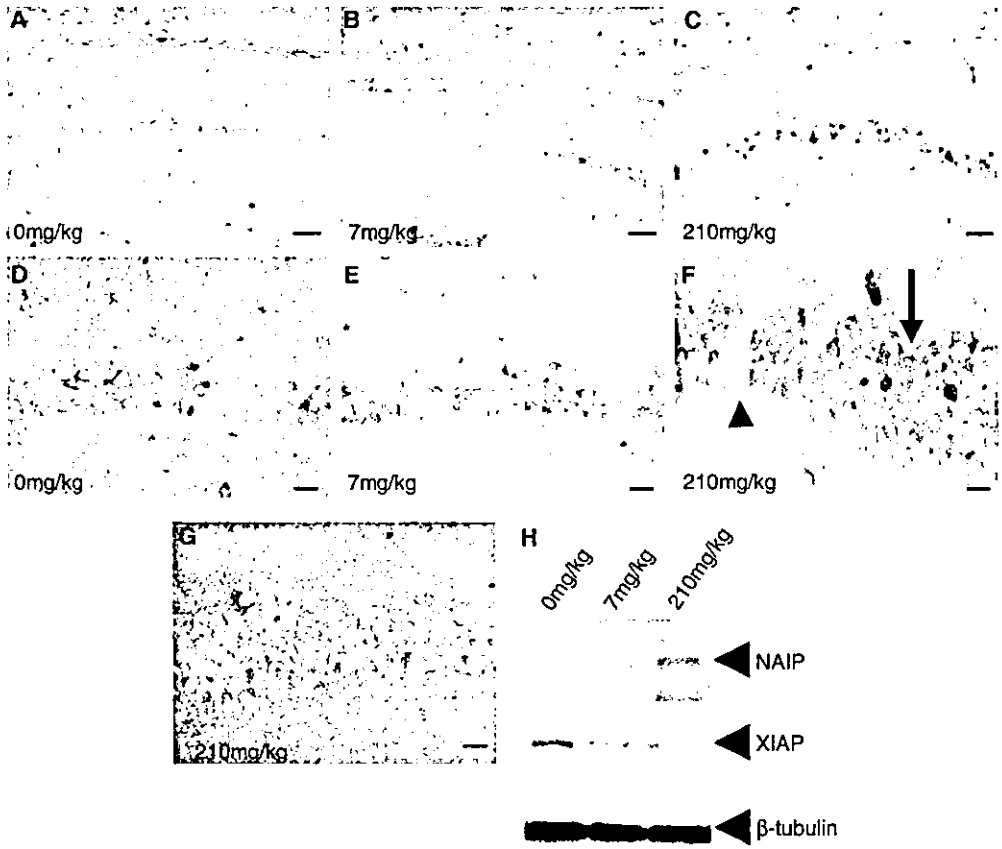

Figure 7 Effect of L-745,870 on expression of neuronal apoptosis inhibitory protein (NAIP) in CA1 neurons of ischemic gerbils. Adult gerbils were treated with L-745,870 and then subjected to forebrain ischemia (bilateral common carotid artery occlusion (BCCAO) for 10 mins; **A–G**). Representative coronal brain sections at the level of the dorsal hippocampus at 72 h (3 days) after reperfusion are shown (**A–G**). Tissues were immunostained with NAIP polyclonal antibody (ME1). Dosages of L-745,870 administered were 0 mg/kg (**A** and **D**), 7 mg/kg (**B** and **E**), and 210 mg/kg (**C**, **F**, and **G**). Scale bar: 100 μm in lower magnification (× 100; **A–C**); 20 μm in higher magnification (× 400; **D–G**). (**F**) Arrow and arrowhead indicate the NAIP-positive and negative cell, respectively. (**G**) Immunostaining of X-linked inhibitor of apoptosis (XIAP) in CA1 neurons of ischemic gerbil pretreated with L-745,870 (210 mg/kg). (**H**) Western blot analysis of NAIP and XIAP in hippocampus at 72 h (3 days) after ischemia. Upper, middle, and lower panels represent the expression of NAIP, XIAP, and β-tubulin, respectively. Each arrow indicates a position of the protein of interest (NAIP: 150 kDa, XIAP: 47 kDa). Expression of β-tubulin demonstrates equal loading in each lane.

1997; Seshagiri and Miller, 1997; Takahashi *et al*, 1998; Maier *et al*, 2002), while we previously showed that the antiapoptotic effect of NAIP was mediated by the caspase-3-independent pathway (Sakai *et al*, unpublished). Further studies to characterize the molecular mechanisms of NAIP upregulation and subsequent inhibition of oxidative stress-induced cell death would be of benefit.

It is notable that L-745,870 slightly but consistently downregulates the levels of both XIAP and cIAP-1 in differentiated SH-SY5Y cells. Recent studies have shown that a group of the ring finger-containing members of IAP family protein, such as XIAP and cIAP, can function as ubiquitin protein ligases, and regulates the levels of not only their target proteins but also themselves through ubiquitylation (Yang *et al*, 2000; Salvesen and Duckett, 2002). Thus, it is possible that L-745,870 may affect the stability of these IAP proteins via regulating the proteasome-dependent protein degradation. Equally likely is that this compound directly or indirectly modulates the expression of these genes and/or proteins in SH-SY5Y cells. Further studies will be needed to clarify the molecular mechanism underlying this inhibitory effect. Nevertheless, as the downregulation of XIAP and cIAP-1 is expected to exert the opposite effect to antiapoptosis, the decreases in XIAP and cIAP-1 observed in this study may not be a primary determinant for the antiapoptotic function associated with L-745,870.

We also showed that L-745,870 attenuated ischemia-induced CA1 neuronal cell death with concomitant increase in the NAIP expression in rescued CA1 neurons. Indeed, selective upregulation of NAIP might mediate a broad range of protection against oxidative stress-induced cell death. For example, a previous study has shown that the small molecule alkaloid, K252a, which is structurally quite different from L-745,870, upregulated NAIP levels and exerted a significant protective effect against ischemic damage in hippocampal CA1 neurons (Xu *et al*, 1997).

In conclusion, the dopamine D4 receptor antagonist, L-745,870, exerts a potent neuroprotective effect against ischemia-induced cell death via increases in NAIP. Since L-745,870 is clinically well tolerated (Bristow *et al*, 1997), this compound may represent an effective therapeutic strategy for the clinical prevention of neuronal cell death after ischemia. Future studies not only on the molecular mechanism by which L-745,870 induces the NAIP expression but also on the effectiveness of this compound in various ischemic conditions will clarify therapeutic potentials of L-745,870 in the treatment of several types of acute as well as chronic neurodegenerative diseases caused by oxidative stress. Further, our NAIP-ELISA-based drug screening may facilitate the discovery of novel neuroprotective compounds.

Acknowledgements

The authors thank Dr Kenji Yamamoto and all the members of our laboratory for their scholarly input.

References

Baldessarini RJ (1997) Dopamine receptors and clinical medicine. In: *The dopamine receptors* (Neve KA, Neve RL, eds), Totowa, NJ: Humana, 457–98

Bristow LJ, Kramer MS, Kulagowski J, Patel S, Ragan CI, Seabrook GR (1997) Schizophrenia and L-745,870, a novel dopamine D4 receptor antagonist. *Trends Pharmacol Sci* 18:186–8

Chan PH (1994) Oxygen radicals in focal cerebral ischemia. *Brain Pathol* 4:59–65

Crocker SJ, Wigle N, Liston P, Thompson CS, Lee CJ, Xu D, Roy S, Nicholson DW, Park DS, MacKenzie A, Korneluk RG, Robertson GS (2001) NAIP protects the nigrostriatal dopamine pathway in an intrastriatal 6-OHDA rat model of Parkinson's disease. *Eur J Neurosci* 14: 391–400

Crowther JR (1995) *ELISA: theory and practice.* Totowa, NJ: Humana

Deveraux QL, Takahashi R, Salvesen GS, Reed JC (1997) X-linked IAP is a direct inhibitor of cell-death proteases. *Nature* 388:300–4

Deveraux QL, Roy N, Stennicke HR, Van Arsdale T, Zhou Q, Srinivasula SM, Alnemri ES, Salvesen GS, Reed JC (1998) IAPs block apoptotic events induced by caspase-8 and cytochrome *c* by direct inhibition of distinct caspases. *EMBO J* 17:2215–23

Friedlander RM (2003) Apoptosis and caspases in neurodegenerative diseases. *N Engl J Med* 348:1365–75

Gavrilov DK, Shi X, Das K, Gilliam TC, Wang CH (1998) Differential SMN2 expression associated with SMA severity. *Nat Genet* 20:230–41

Graham SH, Chen J (2001) Programmed cell death in cerebral ischemia. *J Cereb Blood Flow Metab* 21:99–109

Grünblatt E, Mandel S, Gassen M, Youdim MBH (1999) Potent neuroprotective and antioxidant activity of apomorphine in MPTP and 6-hydroxydopamine induced neurotoxicity. *J Neural Transm Suppl* 55:57–70

Hsieh-Li HM, Chang JG, Jong YJ, Wu MH, Wang NM, Tsai CH, Li HA (2000) Mouse model for spinal muscular atrophy. *Nat Genet* 24:66–70

Kamakura S, Iwaki A, Matsumoto M, Fukumaki Y (1997) Cloning and characterization of the 5′-flanking region of the human dopamine D4 receptor gene. *Biochem Biophys Res Commun* 235:321–6

Kirino T, Sano K (1984) Fine structural nature of delayed neuronal death following ischemia in the gerbil hippocampus. *Acta Neuropathol (Berlin)* 62:209–18

Krajewski S, Mai JK, Krajewska M, Sikorska M, Mossakowski MJ, Reed JC (1995) Upregulation of bax protein levels in neurons following cerebral ischemia. *J Neurosci* 15:6364–76

Liu XH, Kato H, Chen T, Kato K, Itoyama Y (1995) Bromocriptine protects against delayed neuronal death of hippocampal neurons following cerebral ischemia in the gerbil. *J Neurol Sci* 129:9–14

Love S (1999) Oxidative stress in neurological disease. *Brain Pathol* 9:119–31

Maier JK, Lahoua Z, Gendron NH, Fetni R, Johnston A, Davoodi J, Rasper D, Roy S, Slack RS, Nicholson DW, MacKenzie AE (2002) The neuronal apoptosis inhibitory protein is a direct inhibitor of caspases 3 and 7. *J Neurosci* 22:2035–43

Mattson MP, Duan W, Pedersen WA, Culmsee C (2001) Neurodegenerative disorders and ischemic brain diseases. *Apoptosis* 6:69–81

Monani UR, Sendtner M, Coovert DD, Parsons DW, Andreassi C, Le TT, Jablonka S, Schrank B, Rossol W, Prior TW, Morris GE, Burghes AH (2000) The human centromeric survival motor neuron gene (SMN2) rescues embryonic lethality in Smn(−/−) mice and results in a mouse with spinal muscular atrophy. *Hum Mol Genet* 9:333–9

Nitatori T, Sato N, Waguri S, Karasawa Y, Araki H, Shibanai K, Kominami E, Uchiyama Y (1995) Delayed neuronal death in the CA1 pyramidal cell layer of the gerbil hippocampus following transient ischemia is apoptosis. *J Neurosci* 15:1001–11

Osuga H, Osuga S, Wang F, Fetni R, Hogan MJ, Slack RS, Hakim AM, Ikeda JE, Park DS (2000) Cyclin-dependent kinases as a therapeutic target for stroke. *Proc Natl Acad Sci USA* 97:10254–9

Patel S, Freedman S, Chapman KL, Emms F, Fletcher AE, Knowles M, Marwood R, McAllister G, Myers J, Curtis N, Kulagowski JJ, Leeson PD, Ridgill M, Graham M, Matheson S, Rathbone D, Watt AP, Bristow LJ, Rupniak NM, Baskin E, Lynch JJ, Ragan CI (1997) Biological profile of L-745,870, a selective antagonist with high affinity for the dopamine D4 receptor. *J Pharmacol Exp Ther* 283:636–47

Perrelet D, Ferri A, MacKenzie AE, Smith GM, Korneluk RG, Liston P, Sagot Y, Terrado J, Monnier D, Kato AC

(2000) IAP family proteins delay motoneuron cell death *in vivo*. *Eur J Neurosci* 12:2059–67

Perrelet D, Ferri A, Liston P, Muzzin P, Korneluk RG, Kato AC (2002) IAPs are essential for GDNF-mediated neuroprotective effects in injured motor neurons *in vivo*. *Nat Cell Biol* 4:175–9

Raghupathi R, Graham DI, McIntosh TK (2000) Apoptosis after traumatic brain injury. *J Neurotrauma* 17:927–38

Roy N, Mahadevan MS, McLean M, Shutler G, Yaraghi Z, Farahani R, Baird S, Besner-Johnston A, Lefebvre C, Kang X, Salih M, Aubry H, Tamai K, Guan X, Loannou P, Crawford TO, Jong PJ, Ikeda JE, Korneluk RG, Mackenzie A (1995) The gene for neuronal apoptosis inhibitory protein is partially deleted in individuals with spinal muscular atrophy. *Cell* 80:167–78

Roy N, Deveraux QL, Takahashi R, Salvesen GS, Reed JC (1997) The c-IAP-1 and c-IAP-2 proteins are direct inhibitors of specific caspases. *EMBO J* 16:6914–25

Salvesen GS, Duckett CS (2002) IAP proteins: blocking the road to death's door. *Nat Rev Mol Cell Biol* 3:401–10

Sam EE, Verbeke N (1995) Free radical scavenging properties of apomorphine enantiomers and dopamine: possible implication in their mechanism of action in Parkinsonism. *J Neural Transm Park Dis Dement Sect* 10:115–27

Schapira AH (2002) Neuroprotection and dopamine agonists. *Neurology* 58:9–18

Seshagiri S, Miller LK (1997) Baculovirus inhibitors of apoptosis (IAPs) block activation of Sf-caspase-1. *Proc Natl Acad Sci USA* 94:13606–11

Takahashi R, Deveraux Q, Tamm I, Welsh K, Assa-Munt N, Salvesen GS, Reed JC (1998) A single BIR domain of XIAP sufficient for inhibiting caspases. *J Biol Chem* 273:7787–90

Uberti D, Piccioni L, Colzi A, Bravi D, Canonico PL, Memo M (2002) Pergolide protects SH-SY5Y cells against neurodegeneration induced by H(2)O(2). *Eur J Pharmacol* 434:17–20

Xu DG, Crocker SJ, Doucet JP, St-Jean M, Tamai K, Hakim AM, Ikeda JE, Liston P, Thompson CS, Korneluk RG, MacKenzie A, Robertson GS (1997) Elevation of neuronal expression of NAIP reduces ischemic damage in the rat hippocampus. *Nat Med* 3:997–1004

Xu DG, Bureau Y, McIntyre DC, Nicholson DW, Liston P, Zhu Y, Fong WG, Crocker SJ, Korneluk RG, Robertson GS (1999) Attenuation of ischemia-induced cellular and behavioral deficits by X chromosome-linked inhibitor of apoptosis protein overexpression in the rat hippocampus. *J Neurosci* 15:5026–33

Yamamoto K, Sakai H, Hadano S, Gondo Y, Ikeda JE (1999) Identification of two distinct transcripts for the neuronal apoptosis inhibitory protein gene. *Biochem Biophys Res Commun* 264:998–1006

Yang Y, Fang S, Jensen JP, Weissman AM, Ashwell JD (2000) Ubiquitin protein ligase activity of IAPs and their degradation in proteasomes in response to apoptotic stimuli. *Science* 288:874–7

Yoshikawa T, Minamiyama Y, Naito Y, Kondo M (1994) Antioxidant properties of bromocriptine, a dopamine agonist. *J Neurochem* 62:1034–8

Human Molecular Genetics, 2003, Vol. 12, No. 14 **1671–1687**
DOI: 10.1093/hmg/ddg184

ALS2, a novel guanine nucleotide exchange factor for the small GTPase Rab5, is implicated in endosomal dynamics

Asako Otomo[1,2], Shinji Hadano[1,2], Takeya Okada[2], Hikaru Mizumura[1], Ryota Kunita[1], Hitoshi Nishijima[3], Junko Showguchi-Miyata[2], Yoshiko Yanagisawa[1], Eri Kohiki[1], Etsuko Suga[1], Masanori Yasuda[4], Hitoshi Osuga[1,2], Takeharu Nishimoto[3], Shuh Narumiya[5] and Joh-E Ikeda[1,2,6,*]

[1]Solution Oriented Research for Science and Technology (SORST), Japan Science and Technology Corporation (JST), Tokai University School of Medicine, Isehara, Kanagawa 259-1193, Japan, [2]Department of Molecular Neuroscience, The Institute of Medical Sciences, Tokai University, Isehara, Kanagawa 259-1193, Japan, [3]Department of Molecular Biology, Graduate School of Medical Science, Kyushu University, Fukuoka 812-8582, Japan, [4]Department of Pathology, Tokai University School of Medicine, Isehara, Kanagawa 259-1193, Japan, [5]Department of Pharmacology, Kyoto University Faculty of Medicine, Kyoto 606-8501, Japan and [6]Department of Paediatrics, Faculty of Medicine, University of Ottawa, Ottawa, Ontario K1H 8M5, Canada

Received March 7, 2003; Revised and Accepted May 10, 2003

***ALS2* mutations account for a number of recessive motor neuron diseases including forms of amyotrophic lateral sclerosis, primary lateral sclerosis and hereditary spastic paraplegia. Although computational predictions suggest that *ALS2* encodes a protein containing multiple guanine nucleotide exchange factor (GEF) domains [RCC1-like domain (RLD), the Dbl homology and pleckstrin homology (DH/PH), and the vacuolar protein sorting 9 (VPS9)], the functions of the ALS2 protein have not been revealed as yet. Here we show that the ALS2 protein specifically binds to small GTPase Rab5 and functions as a GEF for Rab5. Ectopically expressed ALS2 protein localizes with Rab5 and early endosome antigen-1 (EEA1) onto early endosomal compartments and stimulates the enlargement of endosomes in cultured cortical neurons. The carboxy-terminus of ALS2 protein carrying a VPS9 domain mediates not only the activation of Rab5 via a guanine-nucleotide exchanging reaction but also the endosomal localization of the ALS2 protein, while the amino-terminal half containing RLD acts suppressive in its membranous localization. Further, the DH/PH domain in the middle portion of ALS2 protein enhances the VPS9 domain-mediated endosome fusions. Taken together, the ALS2 protein as a novel Rab5–GEF, ALS2rab5GEF seems to be implicated in the endosomal dynamics *in vivo*. Notably, a feature common to eight reported ALS2 mutations among motor neuron diseases is the loss of VPS9 domain, resulting in the failure of Rab5 activation. Thus, a perturbation of endosomal dynamics caused by loss of ALS2 rab5GEF activity might underlie neuronal dysfunction and degeneration in a number of motor neuron diseases.**

INTRODUCTION

ALS2 was initially identified as a causative gene for a juvenile recessive form of amyotrophic lateral sclerosis (ALS), termed ALS2 (OMIM 205100), in a Tunisian kindred, and a rare juvenile recessive form of primary lateral sclerosis (PLSJ; OMIM 606353) in both Kuwaiti and Saudi Arabian consanguineous families (1,2). ALS2 is characterized by a loss of upper motor neurons (UMN) and spasticity of limb and facial muscles occasionally associated with several signs of lower motor neuron (LMN) defects (3), whereas PLSJ shows only UMN symptoms with no evidence of denervation (4). Recently,

*To whom correspondence should be addressed at: Department of Molecular Neuroscience, The Institute of Medical Sciences, Tokai University, Isehara, Kanagawa 259-1193, Japan. Tel: +81 463915095; Fax: +81 463914993; Email: joh-e@nga.med.u-tokai.ac.jp

five independent homozygous *ALS2* mutations have been found in four families segregating an infantile-onset ascending hereditary spastic paralysis (IAHSP; OMIM 607225) (5,6) and a single family of a recessive complicated hereditary spastic paraplegia (HSP) (7). All of the *ALS2* mutations are either deletion or splicing site mutations (1,2,5,7). Current analysis of the genotype–phenotype correlations suggest that the truncation of the full-length ALS2 protein (a.k.a. alsin) resulting in the loss-of ALS2 function accounts for UMN degeneration, whereas the short variant of ALS2 resulting from an alternative splicing may be responsible for the phenotypic modulation, and possibly loss of both full-length and short ALS2 proteins might be related to the LMN defects (1,2,8).

Computational predictions have shown that the molecular mass of ALS2 protein (1657 amino acids) is 184 kDa, comprising several putative guanine nucleotide exchange factor (GEF) domains and motifs (1,2). A region in the amino-terminal half of the ALS2 protein is highly homologous to RCC1 (regulator of chromosome condensation) (9), and this is referred to as an RCC1-like domain (RLD) (10). RCC1 is a GEF for Ran (Ras-related nuclear) GTPase (9). The RLD is followed by the Dbl homology (DH) and pleckstrin homology (PH) domains, which are hallmarks for GEFs for Rho (Ras-homologous member) GTPases (11). The carboxy-terminal region contains a vacuolar protein sorting 9 (VPS9) domain, which has been found in a number of Rab5 (Ras-related in brain 5) GEFs including Vps9 (12), Rabex-5 (13), RIN1 (14,15) and RIN2 (16). In addition, eight consecutive MORN (membrane occupation and recognition nexus) motifs (17), whose repetition numbers have previously been reported as two (1) or seven (2), were noted in the region between PH and VPS9 domains.

The small GTPases control a broad spectrum of cellular and molecular processes. Ran GTPase is implicated in nuclear transfer as well as chromatin condensation through the regulation of microtubule assembly (18). The Rho subfamilies are critical regulators of the organization of the actin cytoskeleton (19,20), various signaling cascades (20,21) and neuronal morphogenesis (21–23). Further, the Rab GTPases have emerged as central players for vesicle budding, motility/trafficking and fusion (24). All of these small GTPases act as binary switches by cycling between an inactive (GDP-bound) and an active (GTP-bound) state. GEFs are known to stimulate the exchange of GDP for GTP, thereby generating the active forms of the small GTPases (25). In light of conserved GEF domains, it is tempting to speculate that the ALS2 protein acts as a regulator/activator of particular small GTPases. Notably, a feature common to eight reported mutations in *ALS2* is the loss of the carboxy-terminal VPS9 domain. Thus, a loss of VPS9-associated GEF function, which may result in the obstruction of membrane trafficking and dynamics, could underlie neuronal dysfunction and degeneration. However, none of the molecular features of the ALS2 protein has been revealed as yet, and mechanisms by which a loss of its function leads to a selective dysfunction and degeneration of motor neurons in motor neuron diseases (MNDs) remain unknown.

To delineate the functions of the ALS2 protein *in vivo*, biochemical and cell biological analyses were employed in this study. We demonstrate that the ALS2 protein specifically binds to small GTPase Rab5 and functions as a GEF for Rab5, but not for other 11 small GTPases. In addition, ectopically expressed ALS2 protein shows overlapping localization with either Rab5 or early endosome antigen-1 (EEA1) onto early endosomal compartments, and facilitates the enlargement of endosomes in cultured cortical neurons. The carboxy-terminus of ALS2 protein carrying a VPS9 domain activates Rab5 and mediates the endosomal localization of the ALS2 protein, while the amino-terminal half containing a RLD acts suppressive in its membranous localization. Further, DH/PH domain in the middle portion of the ALS2 protein retains an aggrandizing effect on the VPS9 domain-mediated endosome fusions. These data suggest that the ALS2 protein could function as a Rab5-GEF implicating in the endosome dynamics *in vivo*. The recent identification in a large consanguineous Pakistani HSP kindred of an *ALS2* deletion mutation at VPS9 domain (7) implies that the loss of functional VPS9 domain of the ALS2 protein is sufficient to cause neurodegeneration. Taken together, an obstruction of endosomal dynamics underlies neuronal dysfunction and degeneration in ALS2, PLSJ and HSP, as well as in a number of other MNDs.

RESULTS

The ALS2 protein is a 180 kDa protein and expressed in neurons

To detect the ALS2 protein in tissues, two independent polyclonal antibodies (HPP1024 and HPF1–680) were generated, and used to perform western blotting analysis. HPP1024 and HPF1–680 react with both human and mouse ALS2 proteins (Fig. 1A). Although several cross-reacting bands were observed, a major ~180 kDa common band was detected using these antibodies in mouse and human tissues (Fig. 1A), comparable to the molecular masses of 183 and 184 kDa predicted from murine and human ALS2 amino acid sequences, respectively. Thus, taking the180 kDa protein as the ALS2 protein reveals an expression in the brain that was highest in the cerebellum and lowest in the brain stem and spinal cord, where an expression pattern was similar to those of the *ALS2* mRNA as previously reported (1). Expression of the ALS2 protein in non-central nervous system (CNS) was generally low, except for in the liver, in which a 160 kDa protein, in addition to 180 kDa ALS2, was detected using two independent antibodies (HPP1024 and HPF1-680). Whether this 160 kDa protein represents a liver-specific ALS2 variant or a processed form of the intact ALS2 protein is unclear at this stage. The 180 kDa protein was also observed in the human cerebral cortex and cerebellum (Fig. 1A). No band corresponding to the previously described short ALS2 variant (1,2) was observed (data not shown).

Immunohistochemical analysis of the ALS2 protein using HPF1–680 combined with neuronal and glial markers revealed that the ALS2 protein is expressed in various neurons, but not glial cells (data not shown). Representative ALS2-immunoreactive staining of neurons from the motor area of the normal human cerebral cortex, which corresponds to the atrophic areas in the patient with *ALS2* mutation (6), was shown (Fig. 1B). The ALS2 protein mainly distributed in a diffused manner, but several dot or patchy stainings were consistently observed in

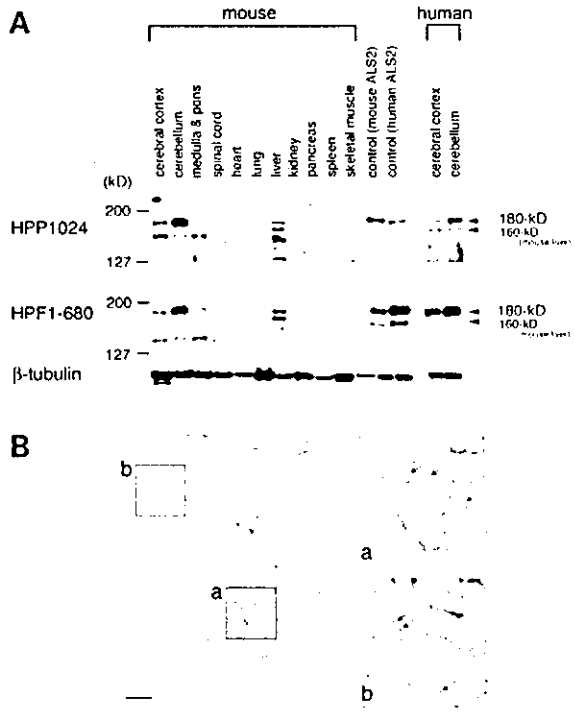

Figure 1. Western blotting and immunohistochemical analyses of the ALS2 protein expression in brain and other tissues in mice and human. (**A**) Western blotting analysis. Two different anti-ALS2 polyclonal antibodies (upper panel; HPP1024, middle panel; HPF1–680) were tested. As positive controls, protein extracts from the COS-7 cells ectopically expressing the full-length human or mouse ALS2 proteins were used. The lower panel represents the expression of β-tubulin to quantify the relative loading. Molecular mass markers are on the left. (**B**) Immunohistochemical analysis of the ALS2 protein using HPF1–680 antibody in the brain sections prepared from human cerebral cortex. The right-hand panels show the enlarged images of neuronal cell body (a) and dendrite (b), respectively. Arrows shown within these enlarged images indicate the typical dot-like stainings, which represent the vesicular localization for the ALS2 protein. Scale bars, 20 μm.

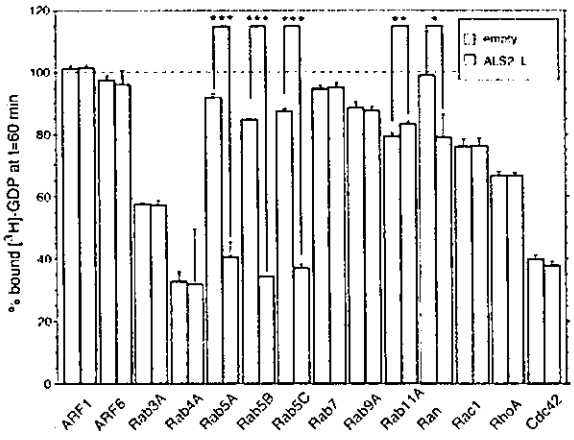

Figure 2. The full-length ALS2 protein accelerates GDP dissociation on members of Rab5 small GTPase family *in vitro*. A total of 14 small GTPases, including ARF1, ARF6, Rab3A, Rab4A, Rab5A, Rab5B, Rab5C, Rab7, Rab9A, Rab11A, Ran, Rac1, RhoA and Cdc42, were subjected to the *in vitro* GDP dissociation assay. Each [^{3}H]GDP-preloaded small GTPase was incubated with the immunoprecipitated FLAG-ALS2_L (gray bars) or FLAG-tag alone (empty; as a control, open bars) from COS-7 cells. The percentage of [^{3}H]GDP bound to each GTPase after 60 min is presented. Each value represents the mean and standard deviation of at least three independent assays. $^{***}P < 0.0001$; $^{**}P < 0.01$; $^{*}P < 0.05$ in *t*-tests.

soma (Fig. 1B-a) as well as in dendrite (Fig. 1B-b), suggesting that the endogenous ALS2 protein localizes not only in the cytosol but also onto vesicular and/or membranous compartments in neurons.

The ALS2 protein acts as a Rab5-specific GEF

The ALS2 protein has been predicted to comprise three GEF domains: RLD, DH/PH and VPS9. To examine ALS2-associated GEF activities, *in vitro* GDP dissociation assays were performed using a variety of bacterially expressed small GTPases [Ran, Rab3A, Rab5A, ARF1 and ARF6 as candidates for RLD (10,26), Rac1, Cdc42 and RhoA as candidates for DH/PH (11), and Rab5A, Rab5B and Rab5C as candidates for VPS9 (12–16)]. Other small GTPases related to the membrane trafficking (24), such as Rab4A, Rab7, Rab9A and Rab11A, were also tested. Immunoprecipitated FLAG-tagged full-length ALS2 protein (ALS2_L) catalyzed [^{3}H]-GDP dissociation on Rab5A, Rab5B and Rab5C exclusively (Fig. 2). This suggests that ALS2_L possesses selective catalytic activity with all the members of Rab5 family. Although ALS2_L showed the weak Ran–GEF activity (Fig. 2), our preliminary assay with the amino-terminal RLD peptide of the ALS2 protein failed to detect any Ran-GEF activities (data not shown). Thus, the Ran-like GEF activity of ALS2_L remains unclear at this stage. In addition, none of the other small GTPases, including three well-characterized Rho-family small GTPases (Rac1, Cdc42 and RhoA) dissociated GDP by incubation with ALS2_L (Fig. 2). These data indicate that full-length ALS2 protein catalyzes GDP dissociation of Rab5 *in vitro*.

ALS2 MORN-VPS9 peptide retains the Rab5-GEF activity

In an effort to map the ALS2 functional domain which confers Rab5-GEF activity, ALS2rab5GEF, amino- and carboxy-terminally truncated ALS2 peptides were generated (Fig. 3A and B), and subjected to the *in vitro* GDP dissociation assay with Rab5A. GDP dissociation was observed with both incubation with full-length ALS2 (ALS2_L) as well as ALS2 peptides comprising 660–1657, 913–1657 or 1018–1657 amino acids, but not with ALS2 peptides of 1251–1657, 1351–1657 or 1–1275 amino acids (Fig. 3C). These results map the region conferring ALS2rab5GEF activity to the interval between 1018 and 1657 amino acids, corresponding to the MORN-VPS9 domains. Lack of either MORN motifs or VPS9 domain resulted in the loss of ALS2rab5GEF activity, indicating that both were necessary for the GEF activity *in vitro*.

To exclude the possibility that cofactors co-immunoprecipitated with ALS2-full length protein and peptides from COS-7 cell extracts were catalyzing the Rab5A-GDP dissociation, the assay was also conducted using bacterially produced GST-fusion ALS2 proteins. GST–ALS2_1018–1657 amino acids-dependent

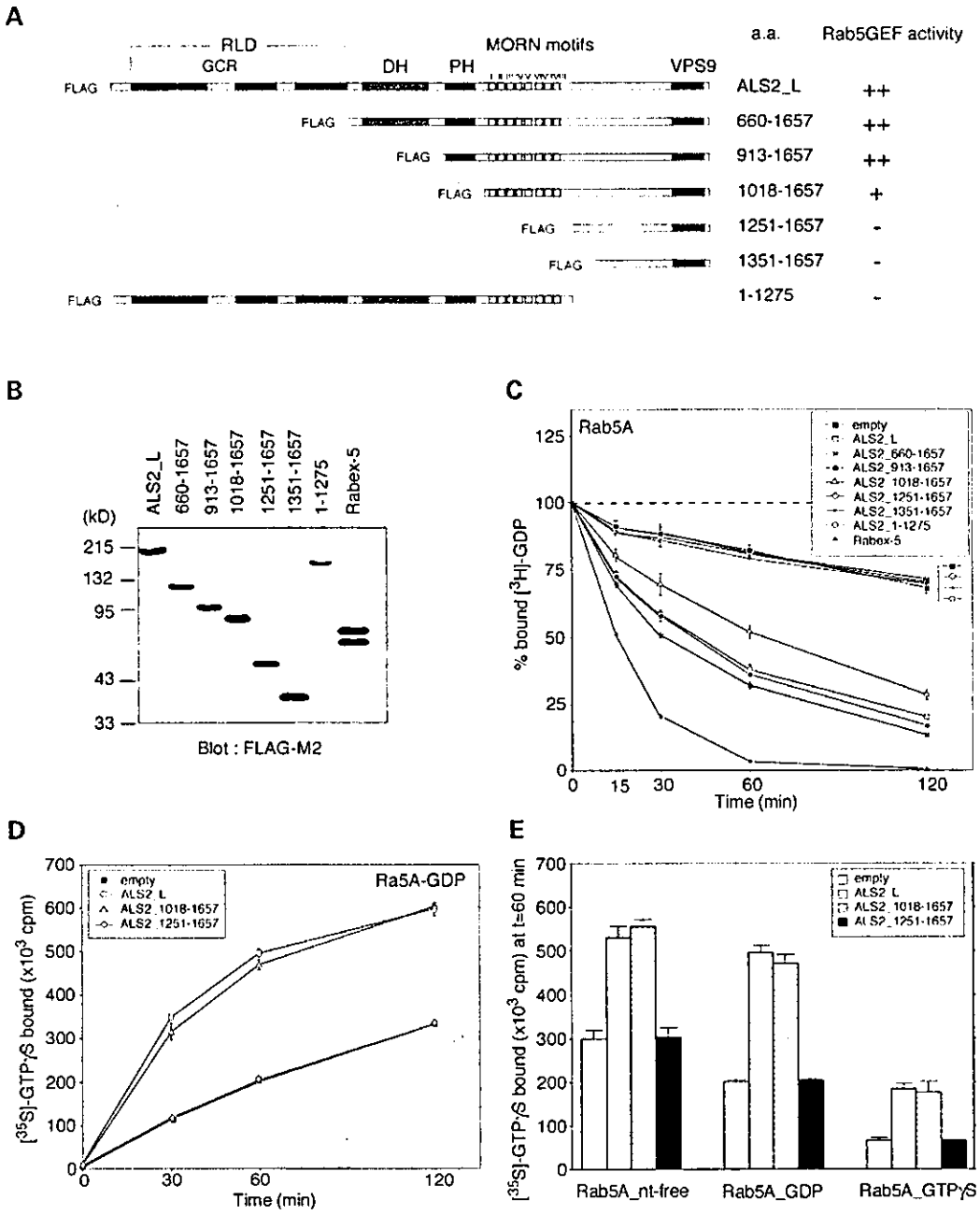

Figure 3. The MORN-VPS9 domain of ALS2 catalyzes Rab5 guanine nucleotide exchange reaction *in vitro*. (**A**) A schematic diagram of the domains and motifs of the ALS2 protein and various truncated mutant ALS2 peptides used for the GDP/GTP exchanging assays *in vitro*. RLD, RCC1-like domain, GCR, glucocorticoid receptor homologous region; DH, Dbl homology domain; PH, pleckstrin homology domain; MORN, membrane occupation and recognition nexus; VPS9, vacuolar protein sorting 9 domain. (**B**) Western blotting analysis of the immunoprecipitated FLAG-tagged full-length ALS2, various ALS2 fragments and Rabex-5 using FLAG-M2 monoclonal antibody. Equivalent amounts of recombinant proteins in the immunoprecipitates were subjected to the GDP/GTP exchanging assays *in vitro*. (**C**) The time-course of the [^{3}H]GDP dissociation on Rab5A induced by incubation with various ALS2 fragments. FLAG-tagged Rabex-5 was used as a positive control. The percentage of [^{3}H]GDP that remained bound on Rab5A at the indicated time points are shown. Each value represents the mean and standard error of three independent assays. (**D**) The time-course of the [^{35}S]GTPγS binding on the GDP-loaded Rab5A in the presence of a various fragments of ALS2. Each value represents the mean and standard error of three independent assays of the bound [^{35}S]GTPγS on Rab5A at the indicated time points. (**E**) Effect of the bound nucleotide-status for Rab5A on the *in vitro* [^{35}S]GTPγS binding activity catalyzed by the ALS2 protein and its truncated peptides. The nucleotide-free (Rab5A_nt-free), GDP-loaded (Rab5A_GDP) or GTPγS-loaded (Rab5A_GTPγS) Rab5A was incubated with [^{35}S]GTPγS in the presence of various ALS2 peptides for 60 min. Counts of the bound [^{35}S]GTPγS on Rab5A are presented. Each value represents the mean and standard deviation of at least three independent assays.

GDP-dissociation was observed, whereas neither GST–ALS2_1251–1657 nor GST–ALS2_1351–1657 amino acids revealed GEF activities with Rab5A (data not shown).

To confirm the ALS2rab5GEF activities, we next examined the ALS2 protein-dependent GTP–Rab5A complex formation by [^{35}S]GTPγS binding to Rab5A *in vitro*. The full-length (ALS2_L) as well as the MORN-VPS9 peptide (ALS2_1018–1657 amino acids) of the ALS2 protein actively exchanged the GDP molecule of the GDP-preloaded Rab5A for [^{35}S]GTPγS, and catalyzed [^{35}S]GTPγS · Rab5A formation in an incubation time-dependent (Fig. 3D). The ALS2 peptide lacking the MORN motifs, ALS2_1251–1657 amino acids, revealed no catalytic activity of either GTP exchange/loading or GDP-dissociation, confirming that the MORN-VPS9 domain spanned a minimum region for the ALS2rab5GEF function. ALS2rab5GEF, residing in the full-length or MORN-VPS9 peptide, actively loaded [^{35}S]GTPγS onto the GDP-bound Rab5A as well as nucleotide-free forms of Rab5A (Rab5A_GDP or Rab5A_nt free), while GTPγS-preloaded Rab5A molecules (Rab5A_GTPγS) were substrates with lower preferentiality (Fig. 3E).

The ALS2 protein interacts directly with Rab5

To examine whether the ALS2 protein directly interacts with Rab5, we carried out the *in vitro* binding assay using the FLAG-M2 pull-down experiment. The amino-terminally FLAG tagged full-length ALS2 protein bound to any form of Rab5A, including Rab5A_nt-free, Rab5A_GDP, and Rab5A_GTPγS, with the strongest binding to the nucleotide-free form of Rab5A (Fig. 4A). To examine the specificity for Rab5A binding and to refine the Rab5A binding region of the ALS2 protein, a series of GST-tagged ALS2-deletion constructs were generated and subjected to the GST pull-down experiments (Fig. 4B and C). GST–ALS2_1018-1657 amino acids, which spans a minimum region for ALS2rab5GEF activity, bound strongly to Rab5A, but not to either Rab4A or Rab11A (Fig. 4C), indicating that the binding is Rab5-specific. Further truncated ALS2 peptides, GST–ALS2_1251–1657 and _1351–1657 amino acids, showed weaker but reproducible Rab5A-binding activity (Fig. 4C), although both peptides no longer retain the GEF activities as mentioned above (Fig. 3C). Similar binding results were obtained from the yeast two-hybrid assay, in which ALS2_1351–1657 amino acids showed an interaction with Rab5A, while ALS2_1018–1351 amino acids, a peptide containing a consecutive MORN motif, did not (data not shown). Thus, a minimum region (1351–1657 amino acids) that needs to establish an interaction between the ALS2 protein and Rab5A is narrower and differs from the ALS2rab5GEF catalytic domain. Nevertheless, the steady interaction between ALS2_1018–1657 amino acids and Rab5A might be essential for the ALS2rab5GEF activity. All the ALS2 peptides tested in this assay showed selective bindings to any forms of Rab5A (Rab5A_nt-free, Rab5A_GDP and Rab5A_GTPγS; Fig. 4C).

Ectopically expressed ALS2 protein exhibits overlapping distribution with Rab5 and EEA1 onto early endosome compartments

To investigate the sub-cellular localization of the ALS2 protein in detail, HeLa cells were transfected with expression construct

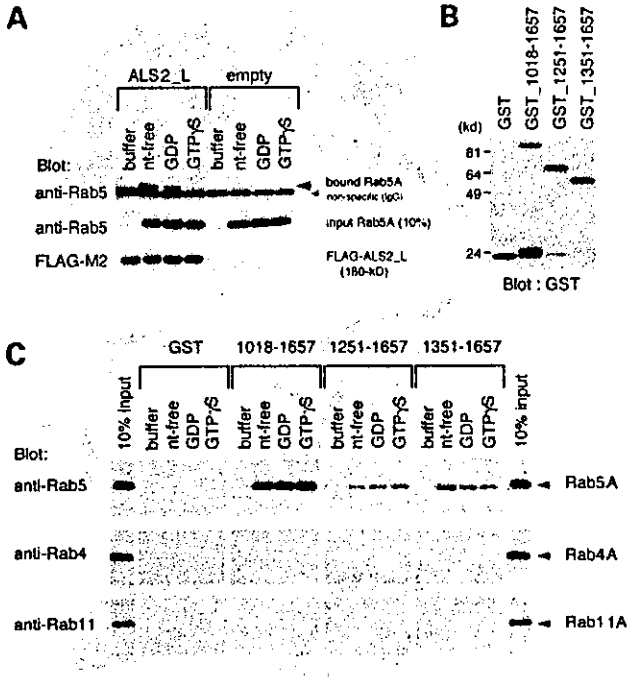

Figure 4. The carboxy-terminal portion of the ALS2 protein containing VPS9 domain is responsible for the direct interaction with Rab5A *in vitro*. (A) *In vitro* Rab5A binding assay using FLAG-tagged full-length ALS2. Nucleotide free (nt-free), GDP-bound (GDP), or GTPγS-bound (GTPγS) forms of Rab5A were incubated with FLAG-M2 beads conjugating FLAG-tagged full-length ALS2 (ALS2_L) or with FLAG-M2 beads alone (empty) as a control. The bound Rab5A was detected by immunoblotting method using anti-Rab5 antibody. Western blotting analyses of the input Rab5A and FLAG-tagged ALS2 were also conducted using anti-Rab5 and FLAG-M2 antibodies, respectively. (B) Western blotting analysis of the purified GST-fusion ALS2 peptides used in the GST pull-down assay. The positions of relative-molecular mass markers are shown on the left. (C) *In vitro* GST pull-down assay. Nucleotide free, GDP-bound or GTPγS-bound forms of Rab5A, Rab4A and Rab11A were incubated with glutathione–Sepharose 4B beads coupled with three different GST-fusion ALS2 peptides or with GST as a control. The bound Rab5A, Rab4A and Rab11A were detected by immunoblotting method using anti-Rab5, anti-Rab4 and anti-Rab11 antibodies, respectively. The '10% input' lanes show the western blotting analysis using 10% of the total amount of each Rab GTPase used in these binding experiments.

expressing full-length and short form of the ALS2 proteins. Ectopically expressed short ALS2 variant distributed rather uniform in cytoplasm and nucleus with some dot-like stainings (Fig. 5A, ALS2_S). In contrast, when the full-length ALS2 protein was expressed, various patterns of the sub-cellular localizations were observed. By analyzing 500 cells expressing the full-length ALS2 protein, more than 90% of the cells harbored the ALS2 proteins in cytoplasm [Fig. 5A, ALS2_L (pattern 1)], while the ALS2 proteins in ~6% of cells localized onto small vesicular structures in the perinuclear region [Fig. 5A, ALS2_L (pattern 2)], and were found the localization of ALS2 onto the enlarged vesicular structures in less than 1% of the cells [Fig. 5A, ALS2_L (pattern 3), arrow]. Interestingly, irrespective of the differences in distribution patterns, ~20% of the cells revealed dense stainings at the leading edges or the cellular peripheries (Fig. 5A and B, arrowheads). To identify the organelles to which the ALS2 protein localized, co-localization

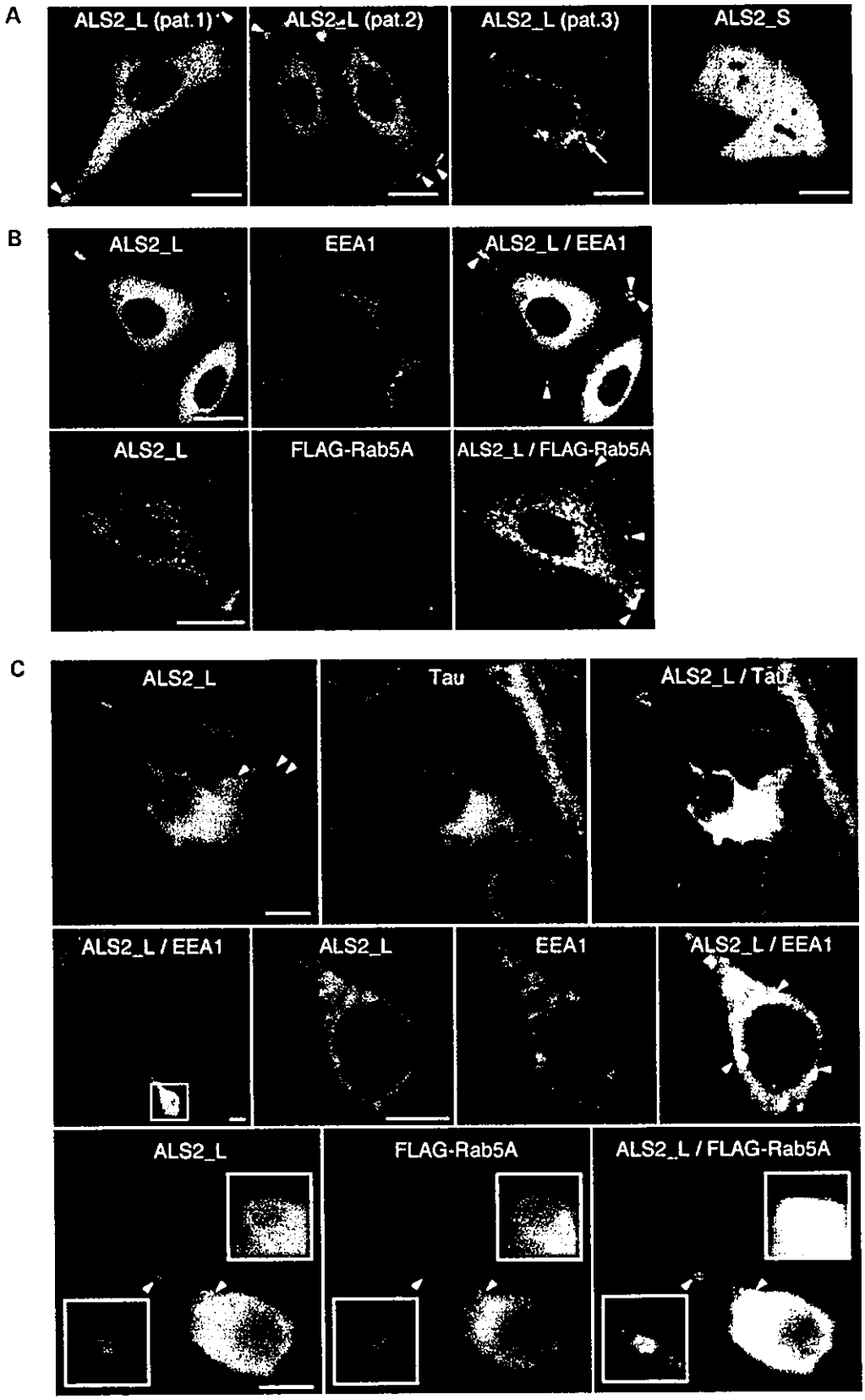
A
ALS2_L (pat.1)
ALS2_L (pat.2)
ALS2_L (pat.3)
ALS2_S
B
ALS2_L
EEA1
ALS2_L / EEA1
ALS2_L
FLAG-Rab5A
ALS2_L / FLAG-Rab5A
C
ALS2_L
Tau
ALS2_L / Tau
ALS2_L / EEA1
ALS2_L
EEA1
ALS2_L / EEA1
ALS2_L
FLAG-Rab5A
ALS2_L / FLAG-Rab5A